Effect of Grain Boundary Stresses on Sink Strength

Chao Jiang[a,*], Narasimhan Swaminatham[b,*], Dane Morgan[a,*], Jie Deng[a], and Izabela Szlufarska[a,*]

[a]Department of Materials Science and Engineering, University of Wisconsin, Madison, WI 53705, USA

[b]Department of Mechanical Engineering, Indian Institute of Technology Madras, Chennai, India

Abstract

Fundamental understanding of the interactions between point defects and grain boundaries (GBs) is critical to designing radiation-tolerant nanocrystalline (nc) materials. An important consideration in this design is sink strength, which quantifies the efficiency of a sink to annihilate point defects. Contrary to the common belief that random high-angle GBs provide the upper limit for rate of defect annihilation, here we show that the sink strength of low-angle GBs can exceed that of high-angle GBs due to the effect of GB stress fields. This surprising finding provides a novel opportunity to enhance the radiation resistance of nc materials through GB engineering.

Keywords: Irradiation, Sink Strength, Grain Boundary

*Corresponding authors

Email: chaopsu@gmail.com (C.J.), n.swaminathan@iitm.ac.in (N.S.), ddmorgan@wisc.edu (D.M.), szlufarska@wisc.edu (I.S.)

Upon exposure to high-energy radiation environments (e.g., due to neutron, electron or ion irradiations), point defects and their complexes are generated in solids in amounts significantly exceeding their equilibrium concentrations. If left unchecked, the accumulation of point defects can lead to undesired consequences such as swelling, embrittlement, and amorphization, which can adversely affect the lifetime of components in nuclear reactors.[1-5] Searches for radiation tolerant materials generally focus on materials with a large number of internal or external interfaces that can act as sinks for irradiation-induced point defects. For instance, the semicoherent interfaces in Cu-Nb nanolayered composites have been shown to be very beneficial for healing radiation damage by trapping and recombining point defects.[4] Another example is the class of nanostructured ferritic steels, which derive their excellent radiation tolerance from a high concentration of nanoprecipitates. In these materials, nanoprecipitate/matrix interfaces provide effective sinks for transmutation products and irradiation-induced defects.[5] A recent study [6] has shown that enhanced radiation resistance can also be exhibited by nanoporous materials, since free surfaces can act as unsaturable defect sinks. In addition, a number of experimental [7,8] and simulation [9-12] studies have shown that bulk nanocrystalline (nc) materials can exhibit enhanced radiation resistance compared to their polycrystalline counterparts due to the presence of a large volume fraction of grain boundaries (GBs). Interestingly, contrary observations regarding the effect of grain refinement on radiation tolerance have also been reported.[13,14] The impact of GBs on defect annihilation and radiation resistance is the focus of our study.

The efficiency of an interface in annihilating point defects can be quantified by its sink strength, which is one of the central parameters in the rate theory models of radiation

resistance.[11,15,16] The higher the sink strength, the slower the defect accumulation rate in a material under irradiation. For a nc material, the GB sink strength increases with decreasing grain diameter R. From the kinetic point of view, a small R is thus beneficial for radiation tolerance. However, small grain size also means a large volume fraction of GB, whose excess energy can destabilize the crystalline lattice and provide a thermodynamic driving force towards grain growth and/or crystalline-to-amorphous transformation. To utilize the great potential of nanocrystalline solids as a new class of radiation resistant materials, it is therefore necessary to understand and control the intricate balance between the GB energy and GB's ability to annihilate defects.[17,18]

For a given grain size, the GB area is approximately independent of the GB type. However, the specific GB energy g_{GB} varies with the GB misorientation. According to the Read-Shockley model,[19] g_{GB} initially increases with the tilt angle of a GB (for low angles) and then reaches an approximately constant value for high-angle GBs. Consequently, from the thermodynamic point of view, a large number of low-angle GBs in a sample would increase its thermal and radiation resistance, because it would reduce the material's overall energy and increase its structural stability. However, due to the fact that tilt GBs with small misorientation angles contain a lower dislocation density than GBs with larger angles, one would expect that low-angle GBs are poor sinks for point defects and their presence will reduce the ability of a material to resist radiation. In this Letter, we demonstrate that the ability of low-angle GBs to annihilate point defects can surprisingly be stronger than that of high-angle GBs due to the interactions of the local GB stress field with point defects.

It is known that the sink strength of a GB depends not only on the GB character and on the grain size, but also on the strengths of other internal sinks within a grain (such as voids and dislocations) as well as on the recombination rate among defects within the grains.[20] Coupling between grain size in nc materials and defect recombination rates has been investigated in detail in Ref. 21. To avoid ambiguities and to isolate the effects of GB character alone, we assume that no other internal sinks (e.g. dislocations and voids) exist in a grain and we do not include in our model the effects of mutual recombination among defects within the grains. Under such simplifications, the time evolution of the average point defect concentrations in a single-element material under irradiation is then governed by the following mean-field rate equation

$$\frac{d\overline{c}_a}{dt} = q - k_a D_a (\overline{c}_a - c_a^e), \qquad (1)$$

where q is the defect production rate in dpa/s, $\overline{c}_a$ is the spatially averaged concentration of point defects of type a (interstitial (i) or vacancy (v)), and D_a is defect diffusivity. c_a^e is the equilibrium defect concentration and is assumed to be negligibly small in the present study. k_a is the so-called sink strength for defect a, which has the units of m^{-2}. Note that k_a in Eq. (1) can be due to either homogenously distributed sinks or localized sinks (or both). Assuming no other significant contributions to defect annihilation, Eq. (1) shows that the steady-state defect concentration in a material is inversely proportional to its sink strength as $\overline{c}_a = q/k_a D_a$. Here, the product $k_a D_a$, with the units of 1/s, is the characteristic rate at which point defects can be annihilated by GB sinks.

To illustrate our results on a specific material system, we consider the sink strength of a low-angle symmetric tilt grain boundary (STGB) in fcc Cu. These GBs can

be modeled by a wall of parallel edge dislocations (Fig. 1(a)). The length b of the burgers vector of the geometrically necessary dislocations is related to the lattice parameter a of Cu through the relation $b = a/\sqrt{2}$. The dislocation separation distance h (inverse of dislocation density along the GB) increases with a decreasing tilt angle q according to the following relationship

$$h = \frac{b}{2\sin(q/2)} \approx \frac{b}{q}. \tag{2}$$

While a STGB does not produce long-range stress fields (the stress magnitude decreases exponentially away from the boundary), its local stress field can nevertheless still be non-negligible, which can interact with the point defects in the vicinity of the GB. The stress field of a small-angle STGB can be calculated by superimposing the stress fields of an infinite array of parallel edge dislocations,[22] and in general is comprised of both normal and shear components. Considering only the first-order size effect,[23] we assume that it is the hydrostatic pressure component of the GB stress field that interacts significantly with the volumetric strain of a point defect. Using the isotropic elasticity theory, the elastic interaction energy between a point defect of type α and the stress field of a low-angle STGB can be calculated as (the *x*-*y* coordinate system is defined in Fig. 1(a))

$$E_a = k_B T L_a \frac{p}{h} \frac{\sin(2p\,y/h)}{\cosh(2p\,x/h) - \cos(2p\,y/h)} \tag{3a}$$

$$L_a = \frac{1+n}{1-n} \frac{mb}{3p} \frac{\Delta V_a}{k_B T} \tag{3b}$$

where k_B is the Boltzmann constant, T is the absolute temperature, ν is the Poisson ratio, m is the shear modulus, ΔV_α is the relaxation volume of defect a, and L_a is the

characteristic length of the interaction field between a point defect and an isolated edge dislocation.[23] ΔV_α is a measure of the strength of the elastic interaction between a point defect and a GB under given m and ν and will be computed from atomistic simulations in the present study.

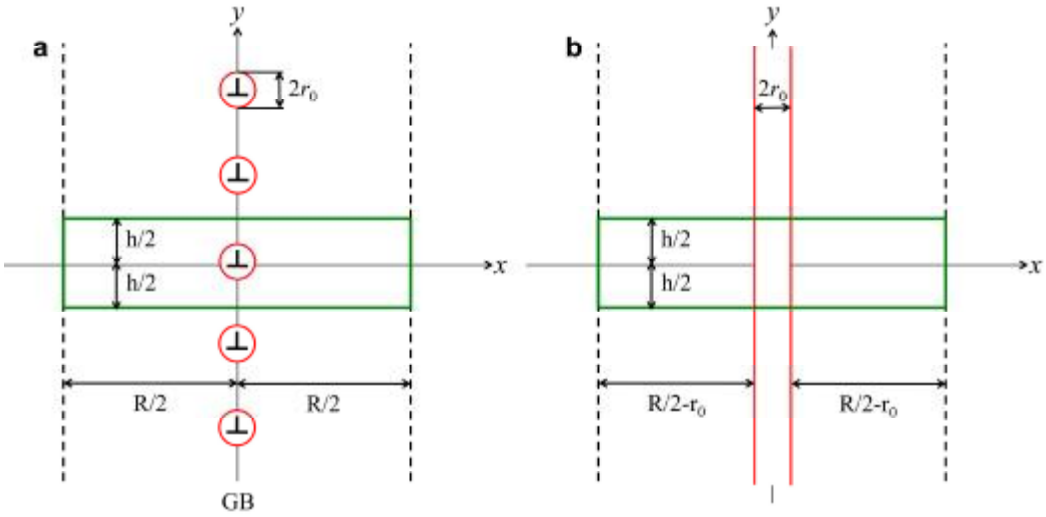

Figure 1. Two-dimensional periodic computational cells employed in this work. (a) A small-angle STGB described by the dislocation model. Each dislocation is represented by a cylinder of radius r_0. (b) A perfect planar sink formed when dislocation cores merge. Periodic boundary conditions are applied along both x and y axis. The green rectangles represent the simulation cell.

For both interstitial and vacancy defects in fcc Cu, we determine their relaxation volumes through a linear least-square fit of elastic interaction energies at pressures of ±5 and ±2 GPa. We calculate the elastic interaction energy E_α as the energy required to move a defect of type α from a stress-free 512-atom fcc Cu supercell to a stressed

supercell corresponding to a given hydrostatic pressure. Density functional theory (DFT) calculations are performed using the all-electron projector augmented wave method [24] within the generalized gradient approximation of Perdew, Burke, and Ernzerhof (PBE), [25] as implemented in Vienna Ab-initio Simulation Package (VASP).[26] The electronic wavefunctions are expanded using a plane-wave basis set with a cutoff energy of 400 eV. For Brillouin zone sampling, a 2×2×2 Monkhorst-Pack k-point mesh is used for the 512-atom supercells. Finally, we obtain ΔV_a by fitting E_α to a linear equation $E_a = p\Delta V_a$ (Fig. 2). The final calculated ΔV_α values are reported in Table 1 together with other parameters for fcc Cu gathered from the literature.[27,28]

Table 1. Parameters for fcc Cu used in the present calculations. The diffusivity of a defect is calculated as $D_a = a^2 n_a e^{-\Delta E_a^m / k_B T}$.

Parameter	Value	Source
Lattice parameter, a	3.615 Å	Ref. 27
Shear modulus, m	47.3 GPa	Ref. 27
Poisson ratio, ν	0.3459	Ref. 27
Relaxation volume of interstitial, ΔV_i	22.44 Å^3	This study
Relaxation volume of vacancy, ΔV_v	-3.80 Å^3	This study
Interstitial migration barrier, ΔE_i^m	0.084 eV	Ref. 28
Vacancy migration barrier, ΔE_v^m	0.69 eV	Ref. 28
Attempt frequency for interstitial migration, ν_i	6.67×10^{12}/s	Ref. 28
Attempt frequency for vacancy migration, ν_v	3.36×10^{13}/s	Ref. 28

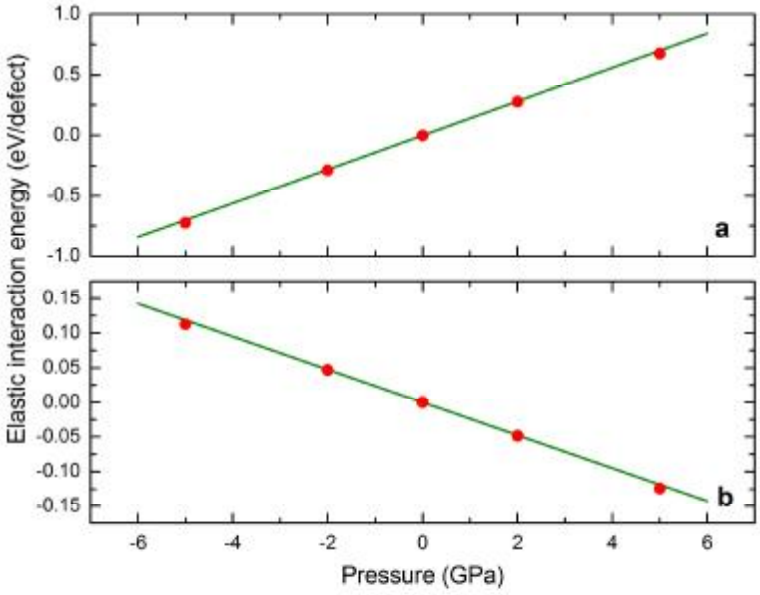

Figure 2. DFT calculated elastic interaction energies of interstitial (a) and vacancy (b) defects in fcc Cu as a function of hydrostatic pressure, fitted to equation $E_a = p\Delta V_a$. The slopes of the fitted lines give the defect relaxation volumes. For interstitial and vacancy, the goodness-of-fit of linear regression is 0.9988 and 0.9978, respectively.

To obtain the sink strength of a low-angle STGB, we find the steady-state solution of the diffusion equation under a continuous irradiation flux

$$\frac{\partial c_a}{\partial t} = q + D_a \left(\nabla^2 c_a + \nabla \cdot \left(c_a \nabla \frac{E_a}{k_B T} \right) \right) = 0 . \quad (4)$$

Due to the GB stress field, in addition to the random diffusion of point defects, there is also a drift term driven by the gradient of elastic interaction energy.[23] In this case, no analytical solution exists and we find numerical solutions using a second-order finite difference scheme. Our computational domain is two-dimensional with periodic boundary conditions applied to both *x* and *y* directions (Fig. 1(a)). The length and height

of the simulation cell are equal to the grain diameter R and the dislocation separation h, respectively. It is known that point defects are absorbed at jogs on climbing dislocations. Here, we assume that dislocation climb in the GB does not have any additional energy barrier that is higher than the migration energy of point defects. In other words, we assume that the long-range diffusion of point defects towards the GB is the rate-limiting step in determining the GB sink strength, not the reaction rate between the defect and the GB sink. The defect concentration at the dislocation core can therefore be fixed at zero. The dislocation core radius r_0 is assumed to be equal to $2b$ in our study. Other choices of r_0 are found to give qualitatively similar results. From the numerically calculated average defect concentration in the matrix, we calculate the GB sink strength as $k_a = q/D_a \overline{c}_a$. Note that our computational approach is different from the one employed by King and Smith, [29] who obtained the GB sink strength from that of an individual dislocation in the GB, multiplied by dislocation density.

When the tilt angle becomes greater than 10°-15°, dislocations overlap and lose their individual identities. These high-angle GBs can be considered as a continuous planar sink (Fig. 1(b)). Furthermore, for high-angle GBs, their local stress field can be neglected due to a complete cancellation of the stress fields of individual dislocations. This trend of a decreasing stress with an increasing grain boundary misorientation angle has been described analytically,[22] verified by our molecular dynamics (MD) simulations (see Supplementary Information), and will be discussed in more detail later in this paper. For a continuous planar sink, analytical solution of its sink strength exists (see Supplementary Information)

$$k_a^{continuous} = \frac{12}{\left(R - 2r_o\right)^2}, \tag{5}$$

where $2r_0$ is the width of the sink. As shown in Fig. S1, our numerically calculated sink strength of the continuous planar sink is in an excellent agreement with the analytical solution, which validates the accuracy of the finite-difference method employed in our study.

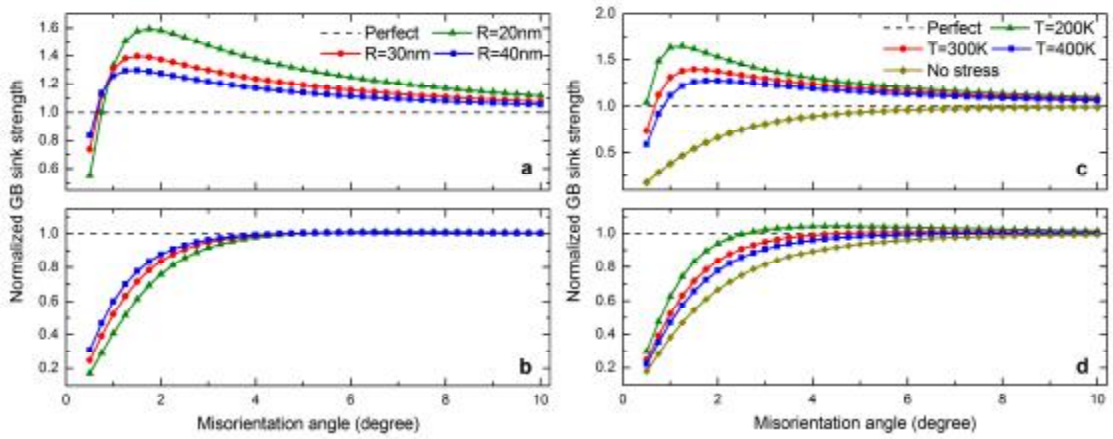

Figure 3. Sink strengths of low-angle STGB as a function of misorientation angle in fcc Cu. All results are normalized by the sink strength of the perfect planar sink. The grain-size dependence of GB sink strengths for interstitial and vacancy at T=300 K are shown in (a) and (b), respectively. The temperature dependence of GB sink strengths for interstitial and vacancy at a grain size of 30 nm are shown in (c) and (d), respectively. The GB sink strengths calculated without considering the effects of GB stress field are also shown for comparison.

Figure 3 shows the calculated sink strengths of low-angle STGBs for both interstitials and vacancies in fcc Cu, all normalized by $k_a^{continuous}$. An interesting finding is

that the GB sink strength for interstitials exhibits a distinct maximum at a rather small misorientation angle ($q_{\max}$ <2º), with $q_{\max}$ shifting towards lower values as the grain size increases (Fig. 3(a)). The height of the maximum, which shows the relative sink strength of a low-angle GB compared to that of a continuous planar sink, is significantly greater than one. This maximum sink strength decreases with increasing grain size, which means that the observed phenomenon will be most pronounced in nc materials. For angles larger than $q_{\max}$, the GB sink strength unexpectedly decreases with increasing q despite the increase of dislocation density in the GB, and approaches the value of the continuous planar sink for large values of q. A similar phenomenon also occurs for C interstitials in SiC (see the Supplementary Information).

For vacancies in Cu (Fig. 3(b)), although a maximum sink strength can still exist, it is much shallower. Above a misorientation angle of around 4º, the GB sink strength for vacancy is almost constant and equal to $k_a^{continuous}$. The less pronounced maximum for vacancies can be explained by the fact that ΔV_α of a vacancy is about six times smaller than that of an interstitial (see Table 1), resulting in a much weaker interaction with the local GB stress field. Our predicted weak GB-vacancy interaction is consistent with a recent atomistic study of bcc Fe.[12] From Figs. 3(c) and 3(d), it can also be seen that the GB sink strength is also temperature-dependent. With increasing temperature, the GB sink strengths for both interstitials and vacancies will approach the same value, which can be calculated using Eq. (1) without considering the GB stress effect (i.e., no drift term).

The relatively flat plot of sink strength vs. GB misorientation angle for vacancies predicted by the present model (Fig. 3(b)) is consistent with existing experimental data on sink strengths. Experimentally, the GB sink strengths are typically measured by

considering interaction of GBs with vacancies. Specifically, by quenching polycrystalline samples from high temperatures, one can obtain a high supersaturation of vacancies in the sample and subsequently one can determine the GB sink strength by measuring the widths of near GB denuded zones.[30-32] Using this methodology, Burke and Stuckey [30] found that, in Al-1.5%Zn alloy, there is very little variation in GB sink strength when q is greater than around 3º. For q below 3º, the GB sink strength decreases significantly. Similarly, Basu and Elbaum [31] observed that all GBs with q ranging from 2° to 50°, with the exception of coherent twin boundaries, are equally effective sinks for vacancies in Al. For the low-angle GBs in Au, Siegel et al. [32] found no significant tendency of the vacancy sink efficiency to decrease with decreasing q in the range $1.8° \le q \le 8.4°$, and they generally found that the vacancy sink efficiencies of low-angle and high-angle GBs (except the special $\Sigma=3$ coherent twin boundary) are rather similar. In all these studies, sink strength is found to remain relatively constant until down to just a few degrees of misorientation angle, which is very consistent with our model predictions (Figs. 3(b)).

To understand the origin the maximums in the GB sink strength vs. misorientation angle curves, we examine how the interaction energy field between an interstitial defect and a low-angle STGB depends on q. We obtain the characteristic length of the interaction field, r_e, as the furthest distance away from the GB plane where the elastic interaction energy is equal to the thermal energy, or $|E_i| = k_B T$. For strong GB-defect interactions ($L_a > h$), r_e can be approximately calculated as

$$r_e \approx \frac{h}{2p} \ln\left(\frac{2p\,L_a}{h}\right) \tag{6}$$

With increasing q, the stress fields of neighboring GB dislocations overlap more strongly, leading to mutual cancellation (Figs. 4(a) and 4(b)). Consequently, r_e decreases monotonically with increasing q (Fig. 4(c)). As shown, Eq. (6) is quite accurate for interstitials due to the large value of L_i.

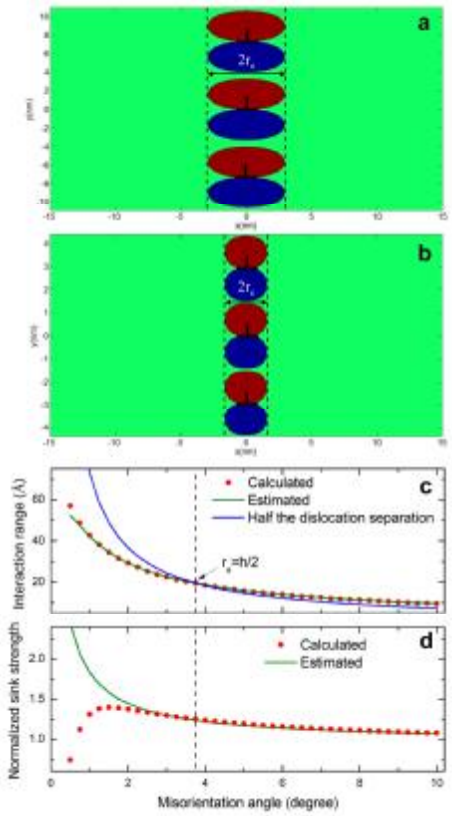

Figure 4. Extent of the elastic interaction between an interstitial defect and a low-angle STGB with misorientation angle of 2° (a) and 5° (b) in Cu. Here T=300 K and R=30 nm. The elastic interaction energy is of opposite sign above and below the dislocation glide plane, respectively. Red and blue regions indicate positive and negative E_i with $|E_i| > k_B T$. The calculated and estimated (see text) characteristic interaction range and GB sink strength for interstitial as a function of misorientation angle are shown in (c) and (d), respectively.

By viewing the GB as a continuous planar sink with an effective width of $2r_e$ due to the interaction field, we can estimate the sink strength of a GB with a local stress field as

$$k_a \approx \frac{12}{\left(R-2r_e\right)^2} \tag{7}$$

As shown in Fig. 4(d), this simple model works very well for larger q values where r_e is greater than half the distance between dislocations (Fig. 4(a)). In this regime, the GB sink strength decreases with increasing q (due to decreasing r_e). As q approaches zero, the dislocation separation approaches infinity (see Eq. (2)), while r_e only approaches a finite value of $L_a/2$. Therefore, for very small q, our model that represents the effects of stresses as an effective GB width will be inapplicable since it is no longer valid to view small-angle GB as a continuous planar sink. In this regime, the GB sink strength increases with increasing q due to increasing dislocation density. The two opposing effects of GB stress field and dislocation density explain the maximums in GB sink strength (Fig. 3).

In order to further support the conclusion that GB sink strength for interstitials decreases with an increasing misorientation angle q, we calculate the interstitial formation energy E_i^f in the bulk region of Cu and in the GBs with different q using MD simulations (details in Supplementary Information). We find that as q increases the range of stress field, the range of affected defect formation energies, and the extent of the defect stabilization all decrease, consistent the conclusion that the GB sink strength for interstitials decreases as q increases due to changing local stress fields. Details are given in the Supplementary Information.

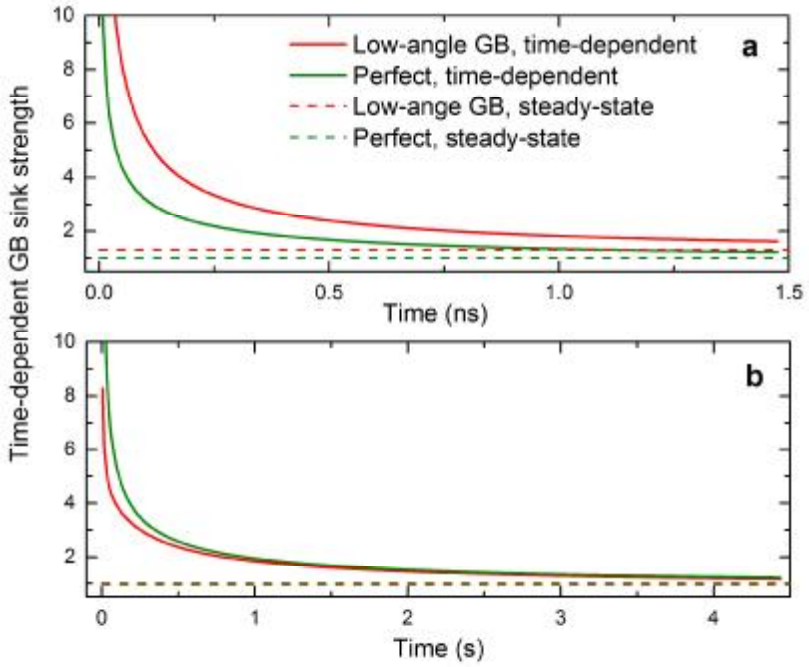

Figure 5. Time-dependent sink strength of a low-angle STGB with a misorientation angle of 3° in comparison with that of the perfect planar sink. Here T=300 K and R=30 nm. All results are normalized by the steady-state sink strength of the perfect planar sink. Results for interstitial and vacancy are shown in (a) and (b), respectively.

Before closing, it is worth pointing out that all the sink strength values reported in this study correspond to the steady state. Since the sink strength is actually also time-dependent, it is important to ask whether time-dependent analysis will lead to the same conclusions as the steady-state solution. To answer this question, we plot in Fig. 5 the time-dependent sink strength (see Supplementary Information) for both a vacancy and an interstitial as a function of time. The time-dependent diffusion equation is solved using the implicit Crank-Nicolson scheme. We find that the GB sink strength is initially very high (infinite at t=0 s) and approaches the steady-state value within a characteristic time

equal to $t \approx R^2/D_a$. Since the diffusivity of interstitials is orders of magnitudes faster than that of vacancies, the steady state is reached much faster for interstitials (Fig. 5(a)) than for vacancies (Fig. 5(b)). For interstitials, the time-dependent sink strength of a low-angle GB is consistently larger than that of the perfect planar sink. For vacancies, the low-angle GB and the perfect planar sink exhibit very similar sink efficiency. These results agree with our steady-state results reported earlier in the paper.

To conclude, we find that the effect of the local stress field around a small-angle GB can dramatically enhance its sink strength. For nanoscale materials, the range of influence of the local GB stress field can be comparable to the grain size. In such a case, the sink strength of a GB with small misorientation angle can surprisingly exceed that of a high-angle GB. Since the irradiation resistance of nc materials is expected to be dominated by GB annihilation, simple analytical models show that the defect concentration is inversely proportional to the sink strength of the GBs.[17] Consequently, the higher sink strength of low-angle GBs translates into lower defect concentrations, which can lead to suppression of amorphization, cluster/loop formation, radiation enhanced creep, and other forms of damage. Furthermore, the small contribution of such GB type to the total free energy is beneficial for the thermodynamic stability of the nc material under radiation. Although special high-angle GBs can also have low energy, their low sink efficiencies are undesirable for radiation tolerance.[31-33] The present finding thus provides an often overlooked avenue for optimizing radiation tolerance of nc materials through GB engineering.[34,35] One effective way to engineer a nanocrystalline material with a large fraction of low-angle GBs is by growth of films on substrates, because texture can be easily introduced during such growth. The degree of

texturing strongly depends on the specific material and on the growth conditions, but in some cases it can approach the value of 100%, leading to the majority of GBs being low-angle. Enhanced GB sink strength, particularly as it is more enhanced for interstitials than for vacancies, may also provide an ability to control radiation induced segregation, which depends on the balance of species dependent fluxes to GB sinks through both vacancies and interstitials.[36] Finally, the discovered effects of stresses on sink strength of interfaces are expected to be relevant in other materials that have a large volume fraction of interfaces, such as ion-implanted multilayer semiconductor structures.

References

[1] de la Rubia TD et al. Multiscale modelling of plastic flow localization in irradiated materials. Nature. 2000;406:871-874.

[2] Odette GR, Lucas GE. Recent progress in understanding reactor pressure vessel steel embrittlement. Radiation Effects Defects Solids. 1998;144:189-231.

[3] Sickafus KE et al. Radiation-induced amorphization resistance and radiation tolerance in structurally related oxides. Nat Mater. 2007;6:217-223.

[4] Misra A, Demkowicz MJ, Zhang X, Hoagland RG. The radiation damage tolerance of ultra-high strength nanolayered composites. JOM. 2007;59:62-65.

[5] Odette GR, Alinger MJ, Wirth BD. Recent Developments in Irradiation-Resistant Steels. Annu Rev Mater Res. 2008;38:471–503.

[6] Bringa EM et al. Are Nanoporous Materials Radiation Resistant?. Nano Lett. 2012;12:3351-3355.

[7] Rose M, Balogh AG, Hahn H. Instability of irradiation induced defects in nanostructured materials. Nucl Instrum Methods Phys Res Sect B. 1997;127-128: 119-122.

[8] Chimi Y et al. Accumulation and recovery of defects in ion-irradiated nanocrystalline gold. J Nucl Mater. 2001;297:355-357.

[9] Bai XM, Voter AF, Hoagland RG, Nastasi M, Uberuaga BP. Efficient annealing of radiation damage near grain boundaries via interstitial emission. Science. 2010;327:1631-1634.

[10] Samaras M, Derlet PM, Van Swygenhoven H, Victoria M. Computer simulation of displacement cascades in nanocrystalline Ni. Phys Rev Lett. 2002;88:125505.

[11] Millett PC, Aidhy DS, Desai T, Phillpot SR, Wolf D. Grain-boundary source/sink behavior for point defects: An atomistic simulation study. Int J Mater Res. 2009;100:550-555.

[12] Tschopp MA et al. Probing grain boundary sink strength at the nanoscale: Energetics and length scales of vacancy and interstitial absorption by grain boundaries in α-Fe. Phys Rev B. 2012;85:064108.

[13] Meldrum A, Boatner LA, Ewing RC. Nanocrystalline zirconia can be amorphized by ion irradiation. Phys Rev Lett. 2002;88:025503.

[14] Lu F et al. Amorphization of nanocrystalline monoclinic ZrO_2 by swift heavy ion irradiation. Phys Chem Chem Phys. 2012;14:12295-12300.

[15] Was GS. Fundamentals of Radiation Materials Science: Metals and Alloys. Springer; 2007.

[16] Brailsford AD, Bullough R. The theory of sink strengths. Philos T R Soc A. 1981;302:87-137.

[17] Shen TD. Radiation tolerance in a nanostructure: Is smaller better?. Nucl Instrum Methods Phys Res Sect B. 2008;266:921-925.

[18] Lu F et al. Size dependence of radiation-induced amorphization and recrystallization of synthetic nanostructured $CePO_4$ monazite. Acta Mater. 2013;61:2984-2992.

[19] Read WT, Shockley W. Dislocation models of crystal grain boundaries. Phys Rev. 1950;78:275-289.

[20] Doan NV, Martin G. Elimination of irradiation point defects in crystalline solids: Sink strengths. Phys Rev B. 2003;67:134107.

[21] Swaminathan N, Morgan D, Szlufarska I. The role of recombination kinetics and grain size on radiation induced amorphization. Phys Rev B. 2013;86:214110.

[22] Hirth JP, Lothe J. Theory of dislocation. McGraw-Hill Book Company; 1968.

[23] Heald PT, Speight MV. Point defect behaviour in irradiated materials. Acta Mater. 1975;23:1389-1399.

[24] Kresse G, Jouber D. From ultrasoft pseudopotentials to the projector augmented-wave method. Phys Rev B. 1999;59:1758-1775.

[25] Perdew JP, Burke K, Ernzerhof M. Generalized gradient approximation made simple. Phys Rev Lett. 1996;77:3865-3868.

[26] Kresse G, Furthmuller J. Efficient iterative schemes for ab initio total-energy calculations using a plane-wave basis set. Phys Rev B. 1996;54:11169-11186.

[27] Wang H, Li M. Ab initio calculations of second-, third-, and fourth-order elastic constants for single crystals. Phys Rev B. 2009;79:224102.

[28] Demkowicz MJ, Hoagland RG, Uberuaga BP, Misra A. Influence of interface sink strength on the reduction of radiation-induced defect concentrations and fluxes in materials with large interface area per unit volume. Phys Rev B. 2011; 84:104102.

[29] King AH, Smith DA. Calculations of sink strength and bias for point-defect absorption by dislocations in arrays. Radiation Effects. 1981;54:169-176.

[30] Burke J, Stuckey D. Dislocation loop-free zones around grain boundaries in quenched aluminum and aluminum alloys. Phil Mag. 1975;31:1063-1080.

[31] Basu BK, Elbaum C. Surface vacancy pits and vacancy diffusion in aluminum. Acta Met. 1965;13:1117-1122.

[32] Siegel RW, Chang SM, Balluffi RW. Vacancy loss at grain boundaries in quenched polycrystalline gold. Acta Met. 1980;28:249-257.

[33] Han WZ, Demkowicz MJ, Fu EG, Wang YQ, Misra A. Effect of grain boundary character on sink efficiency. Acta Mater. 2012;60:6341-6351.

[34] Lu K, Lu L, Suresh S. Strengthening materials by engineering coherent internal boundaries at the nanoscale. Science. 2009;324:349–352.

[35] Tan L, Sridharan K, Allen TR, Nanstad RK, McClintock DA. Microstructure tailoring for property improvements by grain boundary engineering. J Nucl Mater. 2008;374:270-280.

[36] Was GS et al. Assessment of radiation-induced segregation mechanisms in austenitic and ferritic-martensitic alloys. J Nucl Mater. 2011;411:41-50.

Acknowledgments

This research is supported by US Department of Energy, Office of Basic Energy Sciences grant DE-FG02-08ER46493.